

ANGULAR VELOCITY AND POSITION CONTROL OF A PERMANENT MAGNET STEPPER MOTOR.

R. Castro-Linares, Ja. Alvarez-Gallegos and E. Alvarez-Sánchez

Department of Electrical Engineering, CINVESTAV-IPN,

Apdo. Postal 14-740, 07300 México, D.F., México.

Tel.: +52-55-50-61-37-91

Fax: +52-55-50-61-38-66

[rcastro, jalvarez, ejalvare]@mail.cinvestav.mx

Regular Paper

Keywords: Stepping motors, nonlinear systems, sliding control, two-time scale models, signal reconstruction.

Abstract

A control scheme based on the singular perturbations methodology and the sliding mode technique is designed for a permanent magnet (PM) stepper motor. The control scheme designed allows the angular velocity and position of the motor to track some given reference trajectories and it is based on the reconstruction of those signals from direct measurements of the stator currents and stator voltages. Some simulation and experimental results are shown to verify the performance of the control strategy.

1 Introduction

Permanent Magnet (PM) Stepper Motors are electromagnetic incremental motion devices very useful in industrial and research laboratory applications. They are originally designed to provide precise positioning control since they are open-loop stable to any step position and no feedback is needed to control then if the load torque in the rotor is greater than the detent torque. However, they have a step response with overshoot and relatively long settling time. Besides, loss of synchrony appears when steps of high frequency are given [1, 6]. It is thus necessary to develop control schemes to improve the performance of stepper motors. Feedback control methods for this devices are difficult to implement because they are a highly nonlinear systems and it is expensive to have accurate measurement of some of its variables. For example, feedback linearization has been used and implemented in [2], while the concepts of passivity and flatness are applied in [10]. The sliding mode technique is proposed in [4, 5, 7, 11] and the design and use of observers in a control scheme is described in [4, 5, 7, 8].

One area that deserves more research efforts in permanent magnet stepper motor control in the implementation of rotor position measurements. Much research has been focused at the identification of the rotor position signal in closed-loop control strategies. For example, in [3] a sensorless rotor velocity tracking controller is proposed for the nonlinear dynamical

model of a permanent magnet stepper motor activating a mechanical subsystem. In this work, the structure of the electrical subsystem dynamics is exploited in order to reconstruct the rotor position and velocity signals from measurements of currents and voltages in the stator windings. These reconstructed signals are used to synthesize a control strategy to obtain exponential rotor velocity tracking.

In the present paper, a control scheme, based on the singular perturbation methodology and the sliding mode technique, is designed for a PM stepper motor so that their rotor angular velocity and rotor angular position track some given reference trajectories. Following [3], the rotor position and velocity signals are reconstructed from measurement of stator currents and stator voltages and incorporated in the control scheme. The performance of this control strategy was verified through some numerical simulations and experimental tests.

2 Sliding Mode Control

2.1 Two-time scale model of the motor

The basic PM stepper motor consists of a slotted rotor with no windings and a slotted stator with two or more coils. The mathematical model for the PM stepper motor is given by the following singularly perturbed form with $\varepsilon = L$ (see [6] for a detailed explanation and derivation)

$$\begin{aligned} \varepsilon \frac{d\omega}{dt} &= -\frac{k_m}{J} i_a \sin(N_\gamma \theta) + \frac{k_m}{J} i_b \cos(N_\gamma \theta) - \frac{B}{J} \omega \\ &\quad - \frac{k_d}{J} \sin(4N_\gamma \theta) - \frac{\tau_L}{J} \\ \frac{d\theta}{dt} &= \omega \\ \varepsilon \frac{di_a}{dt} &= -Ri_a + k_m \omega \sin(N_\gamma \theta) + v_a \\ \varepsilon \frac{di_b}{dt} &= -Ri_b - k_m \omega \cos(N_\gamma \theta) + v_b \end{aligned} \quad (1)$$

were i_a , i_b and v_a , v_b are the currents and voltages in phases A and B, respectively, ω is the rotor (angular) velocity and θ is the rotor (angular) position. L and R are the self-inductance and resistance of each phase windings, k_m is the motor torque constant, N_γ is the number of rotor teeth, J is

the rotor inertia, B is the viscous friction constant and τ_L is the load torque. The term $k_d \sin(4N_\gamma\theta)$ represents the detent torque due to the permanent rotor magnet interacting with the magnetic material of the stator poles. In the model (1) one neglects the slight coupling between the phases, the small change in the inductance as a function of the rotor position and the variation on inductance due to magnetic saturation (see [2] and the references therein). In the present work one also neglects the detent torque and the load torque (i.e. one sets $k_d = 0$ $N - m$ and $\tau_L = 0$ $N - m$).

When $\varepsilon = 0$, one obtains the value of the currents in stationary state, more precisely

$$\begin{aligned} i_{as} &= \frac{k_m}{R} \omega_s \sin(N_\gamma \theta_s) + \frac{1}{R} v_{as} \\ i_{bs} &= -\frac{k_m}{R} \omega_s \cos(N_\gamma \theta_s) + \frac{1}{R} v_{bs} \end{aligned} \quad (2)$$

Substituting (2) into the first two equations of (1) we obtain the slow reduced subsystem

$$\begin{aligned} \dot{\omega}_s &= -\left(\frac{k_m^2}{JR} + \frac{B}{J}\right) \omega_s - \frac{k_m}{JR} v_{as} \sin(N_\gamma \theta_s) \\ &\quad + \frac{k_m}{JR} v_{bs} \cos(N_\gamma \theta_s) \\ \dot{\theta}_s &= \omega_s \end{aligned} \quad (3)$$

where the subindex s denotes the slow components of the original variables. The fast reduced subsystem is given by $\frac{d\tilde{i}_{af}}{d\tau} = -R\tilde{i}_{af} + v_{af}$, $\frac{d\tilde{i}_{bf}}{d\tau} = -R\tilde{i}_{bf} + v_{bf}$ (see [7] for a detailed computation), where the subindex f represents the fast components of the original variables, and the symbol \sim represents an approximation of these when $\varepsilon \rightarrow 0$ in the fast time scale $\tau = t/\varepsilon$. One can notice that this subsystem is linear and exponentially stable.

2.2 Controller design

Since N_γ is a known parameter, one makes the assignment

$$\begin{aligned} v_{as} &= -\sin(N_\gamma \theta_s) v_s \\ v_{bs} &= \cos(N_\gamma \theta_s) v_s \end{aligned} \quad (4)$$

where v_s is the new scalar control input. When substituting (4) in (3) one obtains

$$\begin{aligned} \dot{\omega}_s &= -\left(\frac{k_m^2}{JR} + \frac{B}{J}\right) \omega_s + \frac{k_m}{JR} v_s \\ \dot{\theta}_s &= \omega_s \end{aligned} \quad (5)$$

Since the fast reduced subsystem is exponentially stable there is no need of a fast control, that is $v_{af} = v_{bf} = 0$.

2.2.1 Angular velocity control

It is desired to track a given angular velocity reference trajectory, $\omega_s^*(t)$, then it is chosen the slow switching function

$$\begin{aligned} \sigma_1(\omega_s, \omega_s^*) &= s_3(\omega_s(t) - \omega_s^*(t)) \\ &\quad + s_2 \int_0^t (\omega_s(\lambda) - \omega_s^*(\lambda)) d\lambda \end{aligned} \quad (6)$$

where s_3 and s_2 are constant real coefficients. The equivalent control method [4] is now used to determine the slow reduced subsystem motion restricted to the slow switching surface defined by $\sigma_1(\omega_s, \omega_s^*) = 0$, obtaining the so-called slow equivalent control

$$\begin{aligned} v_{se} &= \frac{JR}{k_m} \left(\frac{k_m^2}{JR} + \frac{B}{J}\right) \omega_s(t) + \frac{JR}{k_m} \dot{\omega}_s^*(t) \\ &\quad - \frac{s_2}{s_3} \frac{JR}{k_m} (\omega_s(t) - \omega_s^*(t)) \end{aligned} \quad (7)$$

To complete the slow control design, one sets

$$v = v_{se} + v_{sn} \quad (8)$$

where v_{se} is the slow equivalent control (7) which acts when the slow reduced system is restricted to $\sigma_1(\omega_s, \omega_s^*) = 0$, while v_{sn} , the so-called attractive control, acts when $\sigma_1(\omega_s, \omega_s^*) \neq 0$. In this work, v_{sn} is given by [4]

$$\begin{aligned} v_{sn} &= -\frac{JRL_s}{k_m} (\omega_s(t) - \omega_s^*(t)) \\ &\quad - \frac{JRL_s s_2}{k_m s_3} \int_0^t (\omega_s(\lambda) - \omega_s^*(\lambda)) d\lambda \end{aligned} \quad (9)$$

with L_s being a positive constant. The equation that describes the projection of the slow subsystem motion outside $\sigma_1(\omega_s, \omega_s^*) = 0$ can be written as

$$\dot{\sigma}_1(\omega_s, \omega_s^*) = -L_s \sigma_1(\omega_s, \omega_s^*)$$

2.2.2 Angular position control

It is desired to track a given angular position reference trajectory $\theta_s^*(t)$, then, the following switching function is proposed

$$\begin{aligned} \sigma_2(\omega_s, \theta_s, \theta_s^*, \dot{\theta}_s^*) &= a_3(\omega_s(t) - \dot{\theta}_s^*(t)) \\ &\quad + a_2(\theta_s(t) - \theta_s^*(t)) \end{aligned} \quad (10)$$

where a_3 and a_2 are constant real coefficients. The controller is obtained in the same way that for angular velocity control, this is $v = v_{se} + v_{sn}$ with

$$\begin{aligned} v_{se} &= \frac{JR}{k_m} \left(\frac{k_m^2}{JR} + \frac{B}{J}\right) \omega_s(t) + \frac{JR}{k_m} \ddot{\theta}_s^*(t) \\ &\quad - \frac{a_2}{a_3} \frac{JR}{k_m} (\omega_s(t) - \dot{\theta}_s^*(t)) \end{aligned} \quad (11)$$

and

$$\begin{aligned} v_{sn} &= -\frac{JRW_s}{k_m} (\omega_s(t) - \dot{\theta}_s^*(t)) \\ &\quad - \frac{JRW_s a_2}{k_m a_3} (\theta_s(t) - \theta_s^*(t)) \end{aligned} \quad (12)$$

with W_s being a positive constant. The projection of the fast subsystem motion outside the slow switching surface defined by $\sigma_2(\omega_s, \theta_s, \theta_s^*, \dot{\theta}_s^*) = 0$ is described by $\dot{\sigma}_2(\omega_s, \theta_s, \theta_s^*, \dot{\theta}_s^*) = -W_s \sigma_2(\omega_s, \theta_s, \theta_s^*, \dot{\theta}_s^*)$

3 Rotor and Velocity Calculation

Our main objective is to track a reference signal trajectory for the rotor and velocity variables without using mechanical sensors. For doing this, a model-based, open loop estimation algorithm is used to reconstruct the rotor position from the electrical subsystem dynamics. Following [3], a rotor position signal can be calculated from known parameters, stator currents and stator voltages. More specifically, by defining

$$z(t) = [z_1(t) \quad z_2(t)]^T = [\cos(N_\gamma \theta) \quad \sin(N_\gamma \theta)]^T \quad (13)$$

$$p(t) = LI(t) + \frac{k_m}{N_\gamma} z(t) \quad (14)$$

where $I(t) = [i_a(t) \quad i_b(t)]^T$, it can be shown that

$$\dot{p} = V - IR \quad (15)$$

where $V = [v_a \quad v_b]^T$. This last equation is obtained from the time derivatives of $p(t)$ and $z(t)$ and the electrical subsystem in (1). Thus

$$p(t) = \int_0^t [V(\delta) - RI(\delta)] d\delta + p(0) \quad (16)$$

where $p(0)$ is obtained from (14). If the motor is initially aligned (i.e. $\theta(0) = 0$ rad) then

$$p(0) = \begin{bmatrix} Li_a(0) + \frac{k_m}{N_\gamma} \\ Li_b(0) \end{bmatrix} \quad (17)$$

which is a measurable expression since the rotor phase currents i_a and i_b are measurable. Then $p(t)$ can be computed on line from (16) and (17) and an alternative expression for $z(t)$ can be obtained, this is

$$z(t) = \frac{N_\gamma}{k_m} (p(t) - LI(t)) \quad (18)$$

Then, a reconstruction of the rotor position is given by

$$\theta(t) = \frac{1}{N_\gamma} \arctan\left(\frac{z_2(t)}{z_1(t)}\right) \quad (19)$$

In order to calculate the rotor angular velocity $\omega(t)$, a standard backward difference algorithm (Euler type), is used by means of the rotor position signal obtained from (19).

Notice that the reconstruction of the rotor position given by (19) is exact, assuming that the stepper motor is initially aligned. Also, the backward difference algorithm used for the computation of the rotor angular velocity has some drawbacks such as noise. However, this kind of approximation is typically utilized in applications where rotor position is obtained via sensor measurement.

4 Sliding Mode control using reconstructors

4.1 Angular velocity control

In this case, it is considered that the angular position can be measured and just the angular velocity is reconstructed. Thus the switching function is now defined as

$$\begin{aligned} \hat{\sigma}_1(\hat{\omega}, \omega^*) &= s_3(\hat{\omega}(t) - \omega^*(t)) + s_2 \int_0^t (\hat{\omega}(\lambda) - \omega^*(\lambda)) d\lambda \\ &+ s_1 \int_0^t \left(\theta(\lambda) - \int_0^\lambda \omega^*(\rho) d\rho \right) d\lambda \\ &+ s_0 \int_0^t \int_0^\lambda (\theta(\rho) - \int_0^\rho \omega^*(\phi) d\phi) d\rho d\lambda \quad (20) \end{aligned}$$

where $\hat{\omega}$ is the rotor angular velocity reconstructed signal. The control law is then given by $v = v_e + v_n$ where

$$\begin{aligned} v_e &= \frac{JR}{k_m} \left(\frac{k_m^2}{JR} + \frac{B}{J} \right) \hat{\omega}(t) + \frac{JR}{k_m} \dot{\omega}^*(t) \\ &- \frac{s_2 JR}{s_3 k_m} (\hat{\omega}(t) - \omega^*(t)) \\ &- \frac{s_1 JR}{s_3 k_m} \left(\theta(t) - \int_0^t \omega^*(\lambda) d\lambda \right) \\ &- \frac{s_0 JR}{s_3 k_m} \int_0^t \left(\theta(\lambda) - \int_0^\lambda \omega^*(\rho) d\rho \right) d\lambda \quad (21) \end{aligned}$$

is the equivalent control while the attractive control has the form

$$\begin{aligned} v_n &= -\frac{JRL_s}{k_m} ((\hat{\omega}(t) - \omega^*(t))) \\ &- \frac{JRL_s s_2}{k_m s_3} \int_0^t (\hat{\omega}(\lambda) - \omega^*(\lambda)) d\lambda \\ &- \frac{JRL_s s_1}{k_m s_3} \int_0^t \left(\theta(\lambda) - \int_0^\lambda \omega^*(\rho) d\rho \right) d\lambda \\ &- \frac{JRL_s s_0}{k_m s_3} \int_0^t \int_0^\lambda (\theta(\rho) - \int_0^\rho \omega^*(\phi) d\phi) d\rho d\lambda \quad (22) \end{aligned}$$

4.2 Angular position control

Now it is considered that the phase currents of the motor are the only variables that can be measured. The reconstruction of the angular velocity and the angular position are then used and the switching function is now defined as

$$\begin{aligned} \hat{\sigma}_2(\hat{\theta}, \hat{\omega}, \theta^*) &= a_3(\hat{\omega}(t) - \dot{\theta}^*(t)) + a_2(\hat{\theta}(t) - \theta^*(t)) \\ &+ a_1 \int_0^t (\hat{\theta}(\lambda) - \theta^*(\lambda)) d\lambda \\ &+ a_0 \int_0^t \int_0^\lambda (\hat{\theta}(\rho) - \theta^*(\rho)) d\rho d\lambda \quad (23) \end{aligned}$$

where $\hat{\omega}$ and $\hat{\theta}$ are now the rotor angular and velocity reconstructed signals, respectively. The control law is, as before,

given by $v = v_e + v_n$, with v_e being the equivalent control expressed as

$$v_e = \frac{JR}{k_m} \left(\frac{k_m^2}{JR} + \frac{B}{J} \right) \hat{\omega}_r(t) + \frac{JR}{k_m} \ddot{\theta}^*(t) - \frac{a_2}{a_3} \frac{JR}{k_m} \left(\hat{\omega}(t) - \dot{\theta}^*(t) \right) - \frac{a_1}{a_3} \frac{JR}{k_m} \left(\hat{\theta}(t) - \theta^*(t) \right) - \frac{a_0}{a_1} \frac{JR}{k_m} \int_0^t \left(\hat{\theta}(\lambda) - \theta^*(\lambda) \right) d\lambda \quad (24)$$

$$f(t, t_0, t_f) = \left(\frac{t - t_0}{t_f - t_0} \right)^5 \begin{bmatrix} r_1 - r_2 \left(\frac{t-t_0}{t_f-t_0} \right) \\ + r_3 \left(\frac{t-t_0}{t_f-t_0} \right)^2 - r_4 \left(\frac{t-t_0}{t_f-t_0} \right)^3 \\ + r_5 \left(\frac{t-t_0}{t_f-t_0} \right)^4 - r_6 \left(\frac{t-t_0}{t_f-t_0} \right)^5 \end{bmatrix}$$

and an attractive control v_n of the form

$$v_n = -\frac{JRW_s}{k_m} \left(\hat{\omega}(t) - \dot{\theta}^*(t) \right) - \frac{JRW_s a_2}{k_m a_3} \left(\hat{\theta}(t) - \theta^*(t) \right) - \frac{JRW_s a_1}{k_m a_3} \int_0^t \left(\hat{\theta}(\lambda) - \theta^*(\lambda) \right) d\lambda - \frac{JRW_s a_0}{k_m a_3} \int_0^t \int_0^\lambda \left(\hat{\theta}(\rho) - \theta^*(\rho) \right) d\rho d\lambda \quad (25)$$

Remark 1 One may notice that a single and a double integral compensation terms are included in the switching functions (20) and (23). Such terms compensate the error induced by the reconstruction of the rotor angular velocity when an unknown load torque or detent torque appear. However, unknown initial conditions can not be adequately compensated.

5 Simulation and Experimental Results

In this section we present the results obtained through numerical simulations and laboratory experimentation using the equations of the stepper motor described in (1) together with the sensorless sliding mode control proposed in this work, using the nominal values $R = 0.25 \Omega$, $L = 2.3 \text{ mH}$, $k_m = 0.272 \text{ N-m/A}$, $N_\gamma = 50$, $J = 187.2 \times 10^{-6} \text{ Kg-m}^2$, $B = 6 \times 10^{-4} \text{ N-m/rad/s}$, $\tau_L = 0 \text{ N-m}$ and $k_d = 0.1 k_m$. These values correspond to a stepping motor build by Aerotech wired in a bipolar arrange (Aerotech 310 SMB3, Eastern Air Devices Inc.).

To fulfill the objective of making the angular velocity and the angular position of the motor to track a given trajectory, the following trajectory function was used:

$$\varphi^* = \bar{\varphi}_0 + f(t, t_0, t_f) [\bar{\varphi}_f - \bar{\varphi}_0]$$

where t_0 is the initial time, t_f is the final time, $\bar{\varphi}_0$ is an initial value, $\bar{\varphi}_f$ is a final value and $f(t, t_0, t_f)$ is a sufficiently smooth interpolating time polynomial, of the Bézier type that should satisfy

$$f(t_0, t_0, t_f) = 0 \quad f(t_f, t_0, t_f) = 1$$

and is given by [9]

with $r_1 = 252$, $r_2 = 1050$, $r_3 = 1800$, $r_4 = 1575$, $r_5 = 700$ and $r_6 = 126$. For trajectory tracking velocity it was chosen $t_0 = 0 \text{ s}$, $t_f = 0.4 \text{ s}$, $\varphi^* = \omega^*$, $\bar{\varphi}_0 = \bar{\omega}_0 = 0$ and $\bar{\varphi}_f = \bar{\omega}_f = 3 \text{ rad/s}$, while for trajectory tracking position it was chosen $t_0 = 0 \text{ s}$, $t_f = 0.2 \text{ s}$, $\varphi^* = \theta^*$, $\bar{\varphi}_0 = \bar{\theta}_0 = 0$ and $\bar{\theta}_f = 0.031416 \text{ rad}$. For experimental purposes we used $\bar{\varphi}_f = \bar{\omega}_f = 3.8 \text{ rad/s}$.

The initial conditions of the motor variables for both cases, numerical simulation and laboratory experimentation, were fixed to $i_a(0) = 0.0 \text{ A}$, $i_b(0) = 0.0 \text{ A}$, $\omega(0) = 0.0 \text{ rad/s}$ and $\theta(0) = 0.0 \text{ rad}$.

5.1 Simulations results

The coefficients in the switching functions (20) and (23) were selected as $s_0 = 4999$, $s_1 = 69$, $s_2 = 0.165$, $s_3 = 0.0018$, $a_0 = 80$, $a_1 = 13$, $a_2 = 0.165$ and $a_3 = 0.0048$ together with $L_s = 2550$ and $W_s = 1550$.

The time closed-loop plots corresponding to angular velocity tracking and angular position tracking when a load torque is also applied are shown in Fig. 1 and Fig. 2, respectively. From this plots, one can notice the nice response of the system with no overshoot for the angular velocity and the angular position. Also, the control variables are kept within practical limits of operation and the perturbation due to the change in the load torque is adequately compensated.

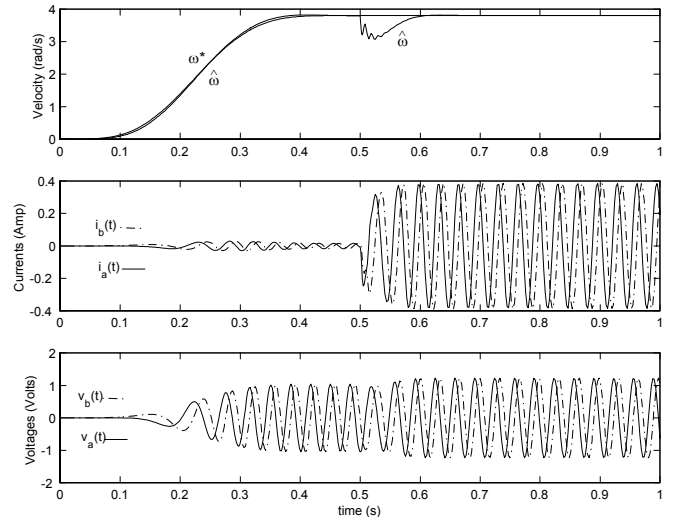


Figure 1: Trajectory tracking for angular velocity.

The figures 3 and 4 show the behavior of the angular velocity and position variables when variations of +30% and +15% are introduced in the nominal values of the viscous friction constant (B) and the phase resistance (R), respectively. We can notice the excellent performance of the control schemes

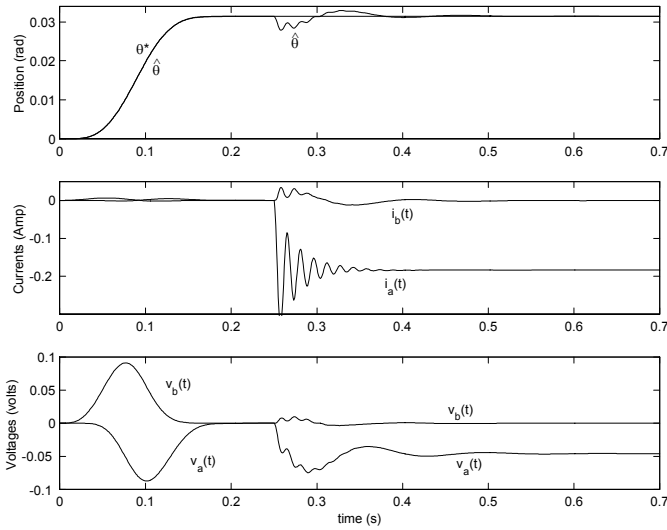


Figure 2: Trajectory tracking for angular position.

when the system has a parametric uncertainty together with a change in the load torque. In all simulations the value of the load torque was changed to $\tau_L = 0.05 \text{ N} - m$ at $t = 0.5 \text{ s}$, for angular velocity, and at $t = 0.25 \text{ s}$, for angular position.

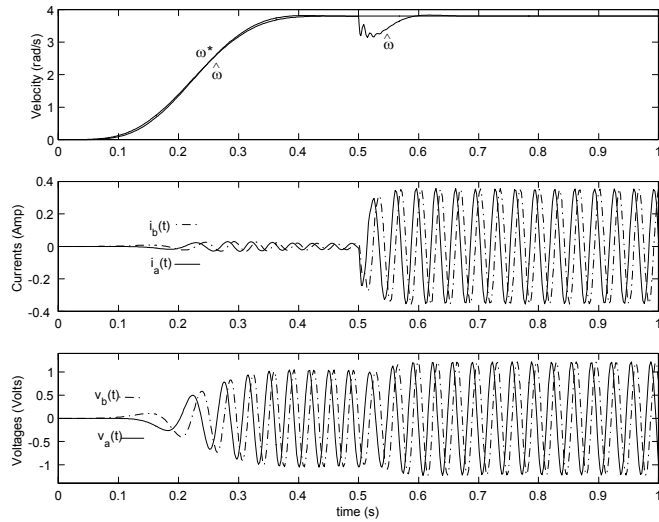


Figure 3: Trajectory tracking for angular velocity (variations in the viscous friction and the phase resistance).

5.2 Experimental Results

In order to experimentally evaluate the performance of the proposed control schemes, a platform was built for the PM stepper motor. The platform consists of an electronic and a control section. The electronic section is formed by a pulse width modulation (PWM) circuit, an isolation stage, a shot sequence stage and a power stage. The control section consists of a personal computer (Pentium II at 120 MHz with 256 Mb in RAM), where the control schemes were implemented using the programming language LabWindows/CVI. Both experiments, this is for angular velocity and angular position control, were made using a sampling period of 1 ms.

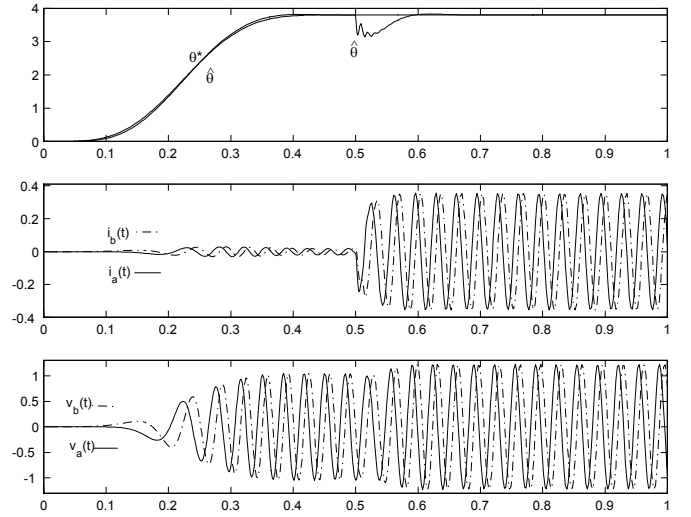


Figure 4: Trajectory tracking for angular position (variations in the viscous friction and the phase resistance).

For the laboratory experimentation the coefficients in the switching functions (20) and (23) were selected as $s_0 = 0$, $s_1 = 2300$, $s_2 = 1.2$, $s_3 = 0.002317$, $a_0 = 50$, $a_1 = 958$, $a_2 = 1.80$ and $a_3 = 0.002448$ together with $L_s = 2299$ and $W_s = 1478.45$.

The time closed-loop responses corresponding to angular velocity tracking and angular position tracking are shown in Fig. 5 and Fig. 6, respectively. The angular velocity and the phase currents were filtered using a third-order Butterworth filter with cut-off frequency at 15 Hz. In these plots one notices that there is a small delay between the reference trajectory and the real signal. This is due to the magnetic detent of the motor which can be considered as an initial load that the control scheme can compensate. Also, the control schemes adequately compensate the uncertainty in the parameters of the model since these are different from the real values.

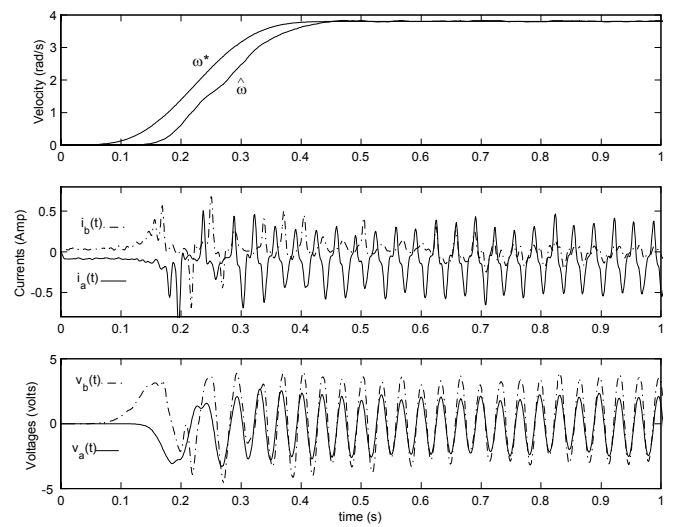


Figure 5: Experimental trajectory tracking for angular velocity.

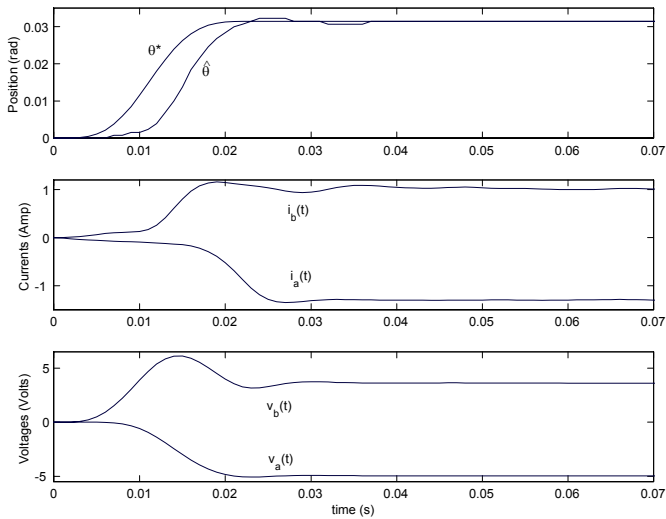


Figure 6: Experimental trajectory tracking for angular position

6 Conclusions

In this article a sensorless sliding mode control scheme was proposed for the trajectory tracking of angular velocity and angular position in a PM stepper motor. For angular velocity tracking only one mechanical sensor is needed to measure the angular position whereas no mechanical sensors are used for angular position tracking. In order to reconstruct the rotor position signal from currents and voltages in the motor's phases, the structure of the electrical subsystem is exploited as proposed in [3]. A calculated rotor velocity signal is computed using a backwards difference algorithm applied to the reconstruction of the rotor position. These calculated mechanical variables are considered as if they were real measurements in the design of the sliding mode controller.

The sliding mode approach used in the design of the control scheme permits to adequately compensate the effect of unknown perturbations (e.g., changes in the load torque and parametric uncertainty). Though no experimental results are shown here for different load torque, it is shown that the control schemes adequately compensate the magnetic detent torque and the uncertainty in the nominal values of the parameters.

Acknowledgments

The third author would like to thank M.C. Victor Hernández for helpful discussions.

References

- [1] P. P. Acarnley. "Stepping Motors: A Guide to Modern Theory", London, UK., (1982).
- [2] M. Bodson, J.N. Chiasson, R.T. Novotnak and R.B. Rekowski. "High-performance nonlinear feedback control of a Permanent Magnet Stepper motor", *IEEE Transactions on Control Systems Technology*, **vol. 1**, No. 1, pp. 5-14, (1993).

- [3] A. Behal, M. Feemster, D. Dawson and A. Mangal. "Sensorless rotor velocity tracking control of the permanent magnet stepper motor", *Proceedings of the 2000 IEEE International Conference on Control Applications*, pp. 150 -155, Anchorage, Alaska, USA, September (2000).
- [4] R. Castro-Linares, Ja. Alvarez-Gallegos and V. Vásquez-López. "Sliding mode control and state estimation for a class of nonlinear singularly perturbed systems", *Dynamics and Control*, **vol. 11**, pp. 25-46, (2001).
- [5] R. Castro, Jm. Alvarez-Gallegos and V. Vásquez-López. "Position control of a stepper motor via a reduced order nonlinear controller-observer scheme", *Proc. of the 4th. European Control Conference 1997*, Track No. TU-Ak2, Brussels, Belgium, July (1997).
- [6] T. Kenjo. "Stepping Motors and Their Microprocessor Controls", Clarendon, Oxford, U.K., (1984).
- [7] J. De León-Morales, R. Castro-Linares, Ja. Alvarez-Gallegos and J. M. Mendivil-Avila. "Controller-observer scheme for a class of nonlinear singularly perturbed systems", *Proceedings of the 40th IEEE Conf. on Dec. and Control*, Orlando, Florida, (2001).
- [8] P. Krishnamurthy and F. Khorrami. "Permanent magnet stepper motor control via position-only feedback", *Proceedings of the American Control Conference*, Anchorage, AK May 8-10, (2002).
- [9] H. Sira-Ramírez. "Differential Flatness: GPI control", *Notes for a course at the University of Delaware*, Delaware, OH, October (2001).
- [10] H. Sira-Ramírez. "Trajectory planning in the regulation of a PM stepper motor: A combined passivity and flatness approach", *Proceedings of the American Control Conference*. Chicago, Illinois, June (2000).
- [11] M. Zribi, H. Sira-Ramirez and A. Ngais. "Static and dynamic sliding mode control schemes for a Permanent Magnet Stepper motor", *International Journal of Control*, **vol. 74**, No. 2, pp. 103-117, (2001).